

## Use of Kramers–Kronig relation in phase retrieval calculation in X-ray spectro-ptychography

Coherent diffraction imaging (CDI) is a method for reconstructing the complex-valued images of objects from their diffraction intensities by using iterative phasing methods. CDI provides information on both the phase shift and the absorption of incident beams due to the interaction with electrons in objects. It is therefore considered that CDI substitutes computational image reconstruction for an image-forming lens. Ptychography, which is a scanning CDI method, is the most practical approach to CDI at third-generation synchrotron facilities since it is free from limitations on the sample size. X-ray ptychography can also provide us with chemical information of a sample by using an X-ray absorption edge, i.e., multiple-energy ptychographic diffraction data are collected in the vicinity of the absorption edge, and then element-specific images are reconstructed, which is often referred to as X-ray spectro-ptychography. An ultimate form of X-ray spectro-ptychography is to reconstruct the X-ray absorption fine structure (XAFS) at the nanoscale. Recently, the XAFS of  $\text{Fe}_3\text{O}_4$  nanoparticles [1] has been reconstructed by soft X-ray spectro-ptychography. Extending this approach to the hard X-ray region will enable us to visualize the chemical state of nanostructures buried within thick samples. However, a limitation of this method is the weak absorption of incident X-rays in the hard X-ray region. In order to improve the convergence of the phase retrieval for complex-valued images in X-ray spectro-ptychography, we proposed the addition of a constraint based on the Kramers-Kronig relation (KKR) to phase retrieval algorithms [2]. In this study, we also performed a proof-of-principle experiment on the reconstruction of near-edge XAFS spectra by X-ray ptychography.

A nanostructured object composed of  $\text{Mn}_2\text{O}_3$  was used as the test sample. A 600-nm-thick  $\text{Mn}_2\text{O}_3$  layer was deposited on a 500-nm-thick  $\text{Si}_3\text{N}_4$  membrane chip, and then both a pattern comprising the characters of “SPring-8” and a square hole were fabricated using a focused ion beam. Figure 1(a) shows a field-emission scanning electron microscopy (FE-SEM) image of the sample. Ptychographic diffraction data of the sample were collected at SPring-8 BL29XUL. Figure 1(b) shows a schematic drawing of the experimental setup. A monochromatic X-ray beam was generated by an in-vacuum undulator device and a Si(111) double-crystal monochromator. Fourteen X-ray energies were selected between 6.530 keV and 6.588 keV, around the *K* absorption edge of Mn. The incident

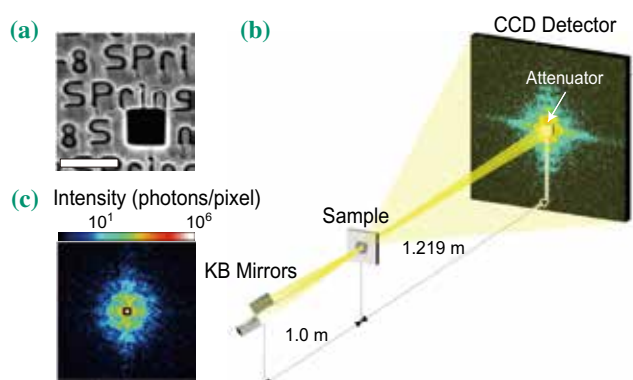


Fig. 1. (a) FE-SEM image of the test sample. The scale bar is 1  $\mu\text{m}$ . (b) Experimental setup at BL29XUL. (c) Coherent diffraction pattern of the sample at 6.554 keV.

X-rays were two-dimensionally focused to a  $\sim 500$  nm (FWHM) spot size using a pair of Kirkpatrick–Baez (KB) mirrors. The sample was positioned at the focal plane and mounted on piezoelectric stages inside a high-vacuum chamber. A diffraction dataset was collected at each position using an in-vacuum front-illuminated CCD detector with a pixel size of  $20 \times 20 \mu\text{m}^2$ , placed 1219 mm downstream of the sample position. To measure the bright field and increase the effective dynamic range of the diffraction intensity, 10- $\mu\text{m}$ -thick Ta with a size of  $640 \times 640 \mu\text{m}^2$  was installed in front of the CCD detector as a semitransparent central stop. The exposure time at each position was 2.8 s and it took  $\sim 1$  h to collect 49 patterns at each X-ray energy, which includes the readout time from the detector and the time required for position correction. The illumination position was corrected at each scanning column by the drift compensation method. This method allows us to radiate the focused X-ray beam with greater accuracy than 10 nm, which was smaller than the pixel size of the reconstructed image. The fluctuation of the incident X-ray energies was much less than 1 eV, which was smaller than the minimum step of the present experiment. Figure 1(c) shows the coherent diffraction pattern of the sample at 6.554 keV. The dynamic range of the diffraction intensity was 1.0 photon/pixel to  $1.9 \times 10^6$  photons/pixel.

Both the sample image and the probe were reconstructed by using a phase retrieval algorithm with and without the KKR constraint. The initial inputs of the object function were constant values and the initial input of the probe was estimated by considering

our experimental parameters. Figures 2(a) and 2(b) show the reconstructed amplitude and phase images at 6.542 keV and 6.554 keV, respectively, after  $2 \times 10^3$  iterations using the KKR constraint every 100 iterations. The reconstructions were in good agreement with the FE-SEM image of the sample. The spatial resolution of the images was determined to be 41.1 nm using the phase retrieval transfer function. The amplitude image showed better contrast at 6.554 keV, which is above the Mn *K* absorption edge. Next, near-edge XAFS spectra were derived from the absorption images. Figures 3(a) and 3(b) show four near-edge XAFS and phase spectra without and with using the KKR constraint, respectively, which were extracted from the  $40 \times 40 \text{ nm}^2$  regions indicated by the arrows in Fig. 2(b). The top spectrum in Fig. 3(a) is the reference spectrum measured in the transmittance mode. Without using the KKR constraint, a strong subpeak appears in addition to the main peak. On the other hand, using the KKR constraint, the intensity of the subpeak decreases and the spectra become closer to the reference spectrum. The RMS error between the reference spectrum and average of the spectra obtained by X-ray spectro-ptychography was improved from 0.232 to 0.178 by using the KKR constraint. It is clear that the KKR constraint works well and provides us with more precise XAFS spectra.

When the range of the X-ray energy in X-ray spectro-ptychography is extended to much higher regions, an extended X-ray absorption fine structure (EXAFS) appears in the absorption images. The EXAFS enables us to directly determine the local

atomic structure around a specific element. The signal of the EXAFS is extremely small compared with that of the near-edge XAFS, and the present reconstruction algorithm with the KKR constraint will be useful for reconstructing the EXAFS signal. In the near future, we believe that the present approach will provide a novel way to understand the relationship between the local atomic structure and the chemical state in unprecedentedly small amounts of materials.

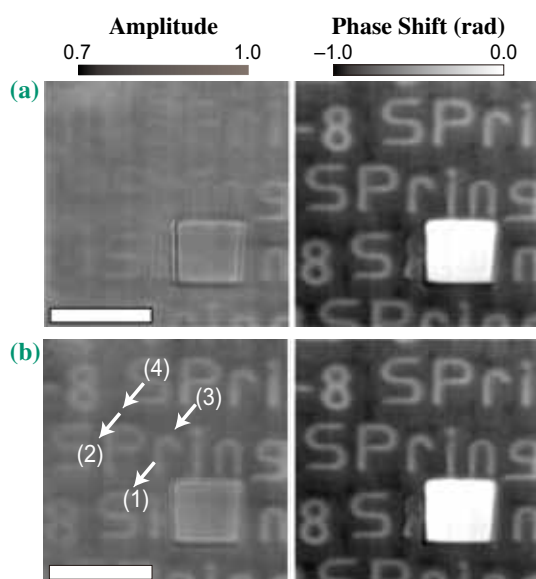


Fig. 2. (a, b) Amplitude (left) and phase (right) images reconstructed from the ptychographic diffraction patterns at (a) 6.542 keV and (b) 6.554 keV. The scale bar is 1  $\mu\text{m}$ .

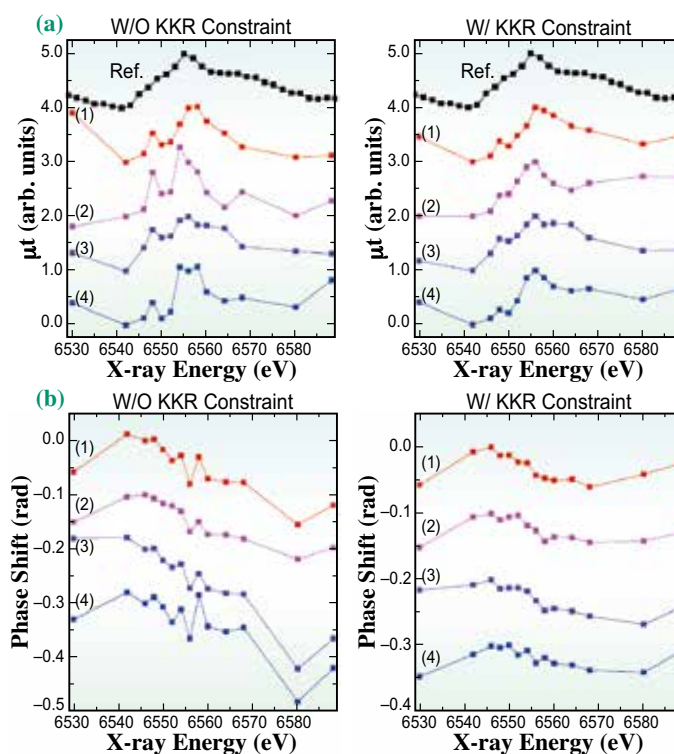


Fig. 3. (a) Near-edge XAFS spectrum of the sample measured in transmittance geometry using a focused X-ray beam (top). Near-edge XAFS spectra reconstructed by X-ray ptychography without (left) and with (right) using the KKR constraint. The spectra were extracted from the  $40 \times 40 \text{ nm}^2$  regions ( $2 \times 2$  pixels) indicated by the arrows in Fig. 2(b). (b) Near-edge phase spectra at the same positions without (left) and with (right) using the KKR constraint.

Yukio Takahashi<sup>a,b\*</sup> and Makoto Hirose<sup>a,b</sup>

<sup>a</sup> Graduate School of Engineering, Osaka University

<sup>b</sup> RIKEN SPring-8 Center

\*Email: takahashi@prec.eng.osaka-u.ac.jp

### References

- [1] X. Zhu *et al.*: Proc. Natl. Acad. Sci. USA **113** (2016) 8219.
- [2] M. Hirose, K. Shimomura, N. Burdet, Y. Takahashi: Opt. Express **25** (2017) 8593.